

A hybrid stochastic method with adaptive time step control for reaction–diffusion systems



Wing-Cheong Lo*, Shaokun Mao

Department of Mathematics, City University of Hong Kong, Kowloon, Hong Kong Special Administrative Region

ARTICLE INFO

Article history:

Received 15 August 2018

Received in revised form 29 November 2018

Accepted 30 November 2018

Available online 12 December 2018

Keywords:

Reaction–diffusion systems

Stochastic simulation

Hybrid method

Biological patterning

ABSTRACT

Randomness often plays an important role in the spatial and temporal dynamics of biological systems. General stochastic simulation methods may lead to excessive computational cost for a system in which a large number of molecules involved. Therefore, multi-scale hybrid simulation methods become important for stochastic simulations. Here we build a spatially hybrid method which couples two approaches: discrete stochastic simulation and continuous stochastic differential equations. In our method, the locations of the interfaces between the two approaches are changing according to the distribution of molecules in a one-dimensional domain. To balance the accuracy and efficiency, the time step of the numerical method for the continuous stochastic differential equations is adapted to the dynamics of the molecules near the adaptive interfaces. The simulation results for a linear system and two nonlinear biological systems in different one-dimensional domains demonstrate the effectiveness and advantage of our new hybrid method with the adaptive time step control.

© 2018 Elsevier Inc. All rights reserved.

Introduction

Many models of biological pattern formation are described by the reaction and diffusion processes. The stochastic behaviors in the processes often have substantial effect when the numbers of the molecules involved in the reactions are relatively small [2,9,24,32]. The mechanisms for achieving robust biological patterns against the negative effects of a noisy environment were discussed in depth in some current studies [3,20,24]. Besides the negative effects, spatial stochastic perturbations might provide positive effects for achieving a robust cell polarization [21] and forming a sharper boundary of gene expression domains [33]. Therefore, the development of a numerical method for studying stochastic effects in biological systems becomes much more important in our future study.

For spatially inhomogeneous systems, the reaction–diffusion stochastic simulation algorithm (SSA) is the popular method to simulate stochastic jumps and reactions to obtain the state of the system after each occurrence of stochastic events [12]. Although the SSA is convenient in terms of its implementation, its computational cost becomes large when the stochastic events in some regions occur significantly more frequently than the events in other regions, as in the case of some regions which have relatively large copy numbers of molecules.

For improving the efficiency, several hybrid methods were proposed for stimulating the stochastic dynamics of spatially inhomogeneous systems [8,10,11,16,23,26–28]. The most usual approach is a spatially hybrid method which combines the

* Corresponding author at: Departments of Mathematics, City University of Hong Kong, HKSAR.

E-mail address: wingclo@cityu.edu.hk (W.-C. Lo).

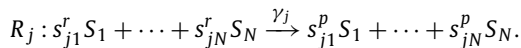
SSA and partial differential equations which provide a mean-field approximation for the stochastic behaviors [13,30]. However, a relatively small stochastic effect in the high concentration region may result in relatively large perturbation in the low concentration region because of the diffusion process in space. So some current studies moved their focus to developing a full stochastic hybrid method [28]. The continuous approach using stochastic partial differential equations can be applied to approximate the stochastic system at a relatively high concentration and provides an additional ability to incorporate the stochasticity in the entire spatial domain. Nevertheless, the coupling of the discrete and continuous approaches and the setting of the time step used in the continuous approach can be improved to be adaptive to different systems for maintaining high accuracy and efficiency. Here, we will focus on these two issues to develop a method which is easily implemented and adaptive to the settings of different one-dimensional reaction–diffusion systems.

In this paper, we build an adaptive spatially hybrid method coupling continuous stochastic differential equations and the SSA. In our hybrid method, the locations of the interfaces between the two numerical methods are adapted to the copy numbers of molecules in each compartment. To balance the accuracy and the efficiency, the time step of the numerical method for the continuous stochastic differential equations is changing according to the dynamics of the molecules near the adaptive interfaces. Then we apply our method to a linear system and two nonlinear biological systems in different one-dimensional domains to verify the effectiveness of our new approach. The simulation results demonstrate that, comparing with the SSA, our hybrid method has a significant improvement in efficiency and the adaptive time step control provides a better balance between the accuracy and efficiency than using fixed time step.

Methods

Spatially inhomogeneous reaction–diffusion system

Consider a system with N molecular species $\{S_1, S_2, \dots, S_N\}$ which are involved in the following M reactions $\{R_1, R_2, \dots, R_M\}$:



Here, s_{ji}^r and s_{ji}^p are the stoichiometric coefficients of the reactant and product species, respectively, and γ_j is the corresponding macroscopic rate constant.

When we are interested in the spatial distribution of the molecules on a one-dimensional domain, the domain with length L can be partitioned into K compartments with uniform length h , where $h = L/K$.

Assumption 1. The diffusion process is fast enough to assume that the subsystem in each compartment is spatially homogeneous. In other words, the size of each compartment must be sufficiently small that diffusive jumps occur more rapidly than reactions and the inhomogeneity inside each compartment can be ignored [14,15,17]. Molecules in different compartments are treated as different species, denoted by

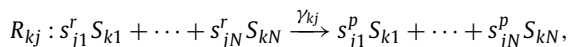
$$\{S_{11}, S_{12}, \dots, S_{ki}, \dots, S_{KN}\},$$

where S_{ki} represents the i th species in the k th compartment. The system state at time t is denoted by $K \times N$ -component vector

$$X(t) = (X_{11}(t), X_{12}(t), \dots, X_{ki}(t), \dots, X_{KN}(t)),$$

where X_{ki} is the number of molecules of S_{ki} .

Assumption 2. We assume that only molecules in the same compartment can react with each other. The M reactions can be considered as $K \times M$ reactions in the spatial system and denoted by R_{kj} , the j th reaction in the k th compartment:



where γ_{kj} is the reaction rate constant of the reaction R_{kj} . The state of the system transfers from one state to another through reaction firing. The net change of the state of the system caused by one occurrence of R_{kj} is denoted as ν_{kj} :

$$\nu_{kj} = (0, \dots, 0, \underbrace{s_{j1}^p - s_{j1}^r, \dots, s_{jN}^p - s_{jN}^r}_{\text{from } ((k-1)N+1)\text{th to } kN\text{th}}, 0, \dots, 0).$$

Assumption 3. Diffusion process is treated as a reaction in which a molecule in one compartment jumps to one of its neighboring compartments. Assume that species S_i diffuses with a diffusion coefficient D_i and the boundary conditions of the one-dimensional domain are considered as reflective boundary conditions at both ends. Therefore, the diffusive jumps obey the following chain reactions:

$$J_{ikL} : S_{1i} \xleftarrow{\frac{D_i/h^2}{D_i/h^2}} S_{2i} \xleftarrow{\frac{D_i/h^2}{D_i/h^2}} S_{3i} \cdots \xleftarrow{\frac{D_i/h^2}{D_i/h^2}} S_{Ki},$$

$$J_{ikR} : S_{1i} \xrightarrow{\frac{D_i/h^2}{D_i/h^2}} S_{2i} \xrightarrow{\frac{D_i/h^2}{D_i/h^2}} S_{3i} \cdots \xrightarrow{\frac{D_i/h^2}{D_i/h^2}} S_{Ki}.$$

We denote the left jump of S_i from the k th compartment by J_{ikL} and the right jump of S_i from the k th compartment by J_{ikR} .

The probability that the reaction R_{kj} will happen in the next time interval $[t, t + dt)$ is $\alpha_{kj}(X(t))dt$, where α_{kj} is called the propensity function of R_{kj} and is defined as

$$\alpha_{kj}(X(t)) = \gamma_{kj} X_{k1}^{s_{j1}^r} X_{k2}^{s_{j2}^r} \cdots X_{kN}^{s_{jN}^r},$$

the probabilities for the jump J_{ikL} and J_{ikR} are $\alpha_{ikL}(X(t))dt$ and $\alpha_{ikR}(X(t))dt$, respectively, where

$$\alpha_{ikL}(X(t)) = \frac{D_i}{h^2} X_{ki}, \text{ for } 1 < k \leq K,$$

$$\alpha_{ikR}(X(t)) = \frac{D_i}{h^2} X_{ki}, \text{ for } 1 \leq k < K.$$

This system can be simulated through the stochastic simulation algorithm (SSA) [12]. At time t , $X(t)$ is given. We first generate two independent random numbers r_1 and r_2 , which are uniformly distributed in $[0, 1]$ and then calculate the next reaction or jump time τ by the following formula

$$\tau = -\frac{1}{\alpha_0} \ln(r_1),$$

where α_0 is the sum of all propensity functions of the jumps J and the reactions R . At time $t + \tau$, a reaction R_{qm} occurs when the smallest q and m exist for an inequality

$$\sum_{k=1}^{q-1} \sum_{j=1}^M \alpha_{kj} + \sum_{j=1}^m \alpha_{qj} \geq r_2 \alpha_0; \tag{1}$$

if q and m do not exist, a left jump $J_{w_1 q_1 L}$ may occur when the smallest q_1 and w_1 exist for an inequality

$$\sum_{k=1}^K \sum_{j=1}^M \alpha_{kj} + \sum_{k=1}^{q_1-1} \sum_{i=1}^N \alpha_{ikL} + \sum_{i=1}^{w_1} \alpha_{iq_1 L} \geq r_2 \alpha_0; \tag{2}$$

if q, m, q_1 and w_1 do not exist, a right jump $J_{w_2 q_2 R}$ may occur when the smallest q_2 and w_2 exist for an inequality

$$\sum_{k=1}^K \sum_{j=1}^M \alpha_{kj} + \sum_{k=1}^K \sum_{i=1}^N \alpha_{ikL} + \sum_{k=1}^{q_2-1} \sum_{i=1}^N \alpha_{ikR} + \sum_{i=1}^{w_2} \alpha_{iq_2 R} \geq r_2 \alpha_0. \tag{3}$$

Then the state $X(t + \tau)$ is updated according to the corresponding state change. This process is repeated until it reaches the stop criterion.

Approximation by stochastic differential equations

Let \bar{u} be X/h which represents the distributions of the molecular concentrations, where $u_{ki} = X_{ki}/h$ in each component. Assume that the numbers of the molecules in each compartment are large, we can approximate the stochastic system by a system of stochastic differential equations (SDE) for \bar{u} [18,22]:

$$du_{ki} = \frac{D_i}{h^2} (u_{(k-1)i} - 2u_{ki} + u_{(k+1)i}) dt + \sum_{j=1}^M r_{kij}(\bar{u}) dt$$

$$+ n_{(k-1)i}(\bar{u}) dW_{(k-1)JR} + n_{(k+1)i}(\bar{u}) dW_{(k+1)JL}$$

$$- n_{ki}(\bar{u}) dW_{kJR} - n_{ki}(\bar{u}) dW_{kJL} + \sum_{j=1}^M n_{kij}(\bar{u}) dW_{kj},$$

for $2 \leq k \leq K - 1,$ (4)

where $r_{kij}(\vec{u})$ is the $[(k-1)N+i]$ th component of $v_{kj}\alpha_{kj}(\vec{u}h)/h$; $n_{kij}(\vec{u})$ is the $[(k-1)N+i]$ th component of $v_{kj}\sqrt{\alpha_{kj}(\vec{u}h)}/h$; $n_{ki}(\vec{u})$ equals to $\sqrt{\frac{D_i}{h^2}}u_{ki}/h$; the variables W 's are the Wiener processes which are independent to each other. For the reflective boundary conditions, when $k=1$, the first term of the right hand side in Eq. (4) is replaced by $\frac{D_i}{h^2}(-u_{1i}+u_{2i})dt$ and the two terms $n_{(k-1)i}(\vec{u})dW_{(k-1)JR}$ and $n_{ki}(\vec{u})dW_{kJL}$ are removed; when $k=K$, the first term of the right hand side in Eq. (4) is replaced by $\frac{D_i}{h^2}(u_{(K-1)i}-u_{Ki})dt$ and the two terms $n_{(k+1)i}(\vec{u})dW_{(k+1)JL}$ and $n_{ki}(\vec{u})dW_{kJR}$ are removed.

For numerical simulation, we simply use the Euler–Maruyama method to calculate the solution for the system of SDE [18]:

$$\begin{aligned}
 u_{ki}(t+\Delta t)-u_{ki}(t) &\approx \frac{D_i}{h^2}(u_{(k-1)i}(t)-2u_{ki}(t)+u_{(k+1)i}(t))\Delta t \\
 &+ \sum_{j=1}^M r_{kij}(\vec{u}(t))\Delta t + n_{(k-1)i}(\vec{u}(t))\sqrt{\Delta t}\zeta_{(k-1)JR} \\
 &+ n_{(k+1)i}(\vec{u}(t))\sqrt{\Delta t}\zeta_{(k+1)JL} - n_{ki}(\vec{u}(t))\sqrt{\Delta t}\zeta_{kJR} \\
 &- n_{ki}(\vec{u}(t))\sqrt{\Delta t}\zeta_{kJL} + \sum_{j=1}^M n_{kij}(\vec{u}(t))\sqrt{\Delta t}\zeta_{kj},
 \end{aligned}$$

(5)

for $2 \leq k \leq K-1$,

where ζ 's are independent standard normal random variables. When $k=1$, the first term of the right hand side in Eq. (5) is replaced by $\frac{D_i}{h^2}(-u_{1i}+u_{2i})\Delta t$, and $n_{(k-1)i}(\vec{u}(t))\sqrt{\Delta t}\zeta_{(k-1)JR}$ and $n_{ki}(\vec{u}(t))\sqrt{\Delta t}\zeta_{kJL}$ are removed; when $k=K$, the first term of the right hand side in Eq. (5) is replaced by $\frac{D_i}{h^2}(u_{(K-1)i}-u_{Ki})\Delta t$, and $n_{(k+1)i}(\vec{u}(t))\sqrt{\Delta t}\zeta_{(k+1)JL}$ and $n_{ki}(\vec{u}(t))\sqrt{\Delta t}\zeta_{kJR}$ are removed.

Here we apply the Euler–Maruyama method as it is easy to be numerically implemented. Actually, we can apply other higher order numerical methods to improve the accuracy [4,18,31]. Although the numerical SDE approach is an efficient method to approximate the stochastic processes with high molecular concentrations, the accuracy may not be high when the number of molecules becomes low. In the later sections, we will develop the hybrid method which couples the SSA and numerical SDE to balance the accuracy and efficiency in the simulation.

Adaptive interfaces between SSA and numerical SDE

To decide a method to capture the advantages of the SSA and numerical SDE, we first consider a way to separate the domain into two regions that satisfies: 1) the method is efficient in the region with large numbers of molecules; 2) the method is accurate in the region with small numbers of molecules. We consider to apply the numerical SDE to approximate the dynamics in the k th compartment if

$$\min_{1 \leq i \leq N; 1 \leq j \leq M} \left\{ \frac{X_{ki}}{|S_{ji}^p - S_{ji}^r|} \right\} > N_{int};$$

(6)

in other compartments, we will apply the SSA for the simulations.

If N_{int} is large, the condition can reduce the probability that the approximation provides a negative number of molecules in the k th compartment after each iteration. A set I_C is defined as a set of all the indexes k satisfying the inequality (6); a set I_D is defined as $\{1, 2, \dots, K\} \setminus I_D$; I_{BR} and I_{BL} are the sets of the left boundary points and the right boundary points, respectively, in all intervals in I_C . A sample of these four sets is illustrated in Fig. 1. Here we simulate the flux between the two regions by the SSA. Therefore, the firing time of the jump between I_C and I_D are stochastic.

In the I_C region, we use the numerical SDE to approximate the stochastic dynamics. If each interval in I_C is larger than one compartment, we use the Euler–Maruyama method, like (5), to build the following iteration for $k \in I_C$:

$$\begin{aligned}
 u_{ki}(t+\Delta t)-u_{ki}(t) &\approx \frac{D_i}{h^2}(u_{(k-1)i}(t)-2u_{ki}(t)+u_{(k+1)i}(t))\Delta t \\
 &+ \sum_{j=1}^M r_{kij}(\vec{u}(t))\Delta t + n_{(k-1)i}(\vec{u}(t))\sqrt{\Delta t}\zeta_{(k-1)JR} \\
 &+ n_{(k+1)i}(\vec{u}(t))\sqrt{\Delta t}\zeta_{(k+1)JL} - n_{ki}(\vec{u}(t))\sqrt{\Delta t}\zeta_{kJR}
 \end{aligned}$$

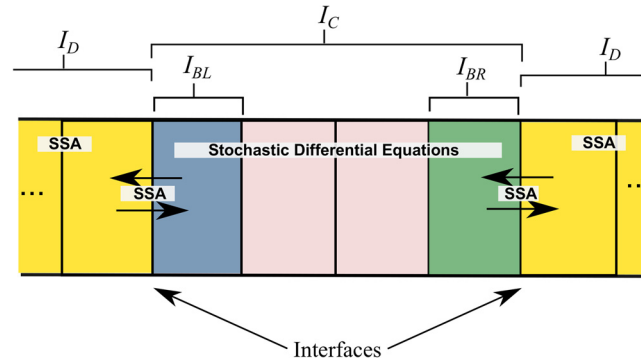


Fig. 1. Illustration of the domain decomposition between the SSA and the stochastic differential equations. I_D (yellow) represents the region for the SSA; I_C (blue, pink, green) represents the region for the SDE; I_{BR} (green) and I_{BL} (blue) are the left boundary points and the right boundary points, respectively, in all intervals in I_C . (For interpretation of the colors in the figures, the reader is referred to the web version of this article.)

$$-n_{ki}(\vec{u}(t))\sqrt{\Delta t}\zeta_{kJL} + \sum_{j=1}^M n_{kij}(\vec{u}(t))\sqrt{\Delta t}\zeta_{kj},$$

for $k \in I_C \setminus (I_{BR} \cup I_{BL})$;

(7)

for $k \in I_{BL}$, the first term of the right hand side in Eq. (7) is replaced by $\frac{D_i}{h^2}(-u_{ki} + u_{(k+1)i})\Delta t$, and $n_{(k-1)i}(\vec{u}(t))\sqrt{\Delta t}\zeta_{(k-1)JR}$ and $n_{ki}(\vec{u}(t))\sqrt{\Delta t}\zeta_{kL}$ are removed; for $k \in I_{BR}$, the first term of the right hand side in Eq. (7) is replaced by $\frac{D_i}{h^2}(u_{(k-1)i} - u_{ki})\Delta t$, and $n_{(k+1)i}(\vec{u}(t))\sqrt{\Delta t}\zeta_{(k+1)JL}$ and $n_{ki}(\vec{u}(t))\sqrt{\Delta t}\zeta_{kJR}$ are removed. If an interval in I_C has only one compartment, we apply Eq. (7) without the diffusion term.

Time step selection for numerical differential equations

The selection of the time step $\Delta t = \Delta t_C$ for the numerical SDE (7) was not discussed in the previous studies of hybrid methods. Based on the study for the efficient τ -selection for the τ -Leaping method [5], we consider that the mean and variance of the relative change of the molecular populations in each iteration is bounded by certain threshold ϵ :

$$| < \Delta_{\Delta t_C} X_{ki} > | \leq \max\{\epsilon X_{ki}, 1\}, \sqrt{\text{var}\{\Delta_{\Delta t_C} X_{ki}\}} \leq \max\{\epsilon X_{ki}, 1\},$$
(8)

for all $k \in I_C$. To satisfy the previous conditions and the condition for the stability of central difference scheme [18]

$$\Delta t_C \leq \Delta t_0 = \min_{1 \leq i \leq N} \left\{ \frac{h^2}{2D_i} \right\},$$

we obtain the following setting for Δt_C selection:

$$\Delta t_C = \min_{1 \leq i \leq N, k \in I_C} \left\{ \frac{\max\{\epsilon h u_{ki}, 1\}}{\mu_{ki}(\vec{u})}, \frac{(\max\{\epsilon h u_{ki}, 1\})^2}{\sigma_{ki}(\vec{u})}, \Delta t_0 \right\}$$
(9)

where

$$\mu_{ki}(\vec{u}) = \frac{D_i}{h^2} (u_{(k-1)i}(t) - 2u_{ki}(t) + u_{(k+1)i}(t))h + \sum_{j=1}^M r_{kij}(\vec{u}(t))h,$$

and

$$\sigma_{ki}(\vec{u}) = \frac{D_i}{h^2} (u_{(k-1)i}(t) + 2u_{ki}(t) + u_{(k+1)i}(t))h + \sum_{j=1}^M (n_{kij}(\vec{u}(t))h)^2,$$

for $k \in I_C \setminus (I_{BR} \cup I_{BL})$. For $k \in I_{BL}$, the first terms of the right hand sides of $\mu_{ki}(\vec{u})$ and $\sigma_{ki}(\vec{u})$ are replaced by

$$\frac{D_i}{h^2}(-u_{ki} + u_{(k+1)i})h \text{ and } \frac{D_i}{h^2}(u_{ki} + u_{(k+1)i})h, \text{ respectively;}$$

for $k \in I_{BR}$, the first terms of the right hand sides of $\mu_{ki}(\vec{u})$ and $\sigma_{ki}(\vec{u})$ are replaced by

$$\frac{D_i}{h^2}(u_{(k-1)i} - u_{ki})h \text{ and } \frac{D_i}{h^2}(u_{(k-1)i} + u_{ki})h, \text{ respectively.}$$

If ϵ is much less than 1, our time step setting can guarantee that the relative changes of the numbers of the molecules are small enough to ensure the numerical stability for the approximation. In the numerical tests, we will take $\epsilon = 0.1$ which is small enough to ensure the numerical stability of the Euler–Maruyama method.

It is worth to remark that although the time step size Δt_C is controlled to reduce the relative error, a negative value may still appear in the iteration (7) with small probability. When a negative value appears, the time step Δt_C can be reduced through dividing by two; if the negative value still exists after Δt_C decreases, the process can be repeated until the negative value does not exist in the iteration (7).

When a jump of a molecule (the process is modeled by the SSA) happens across an interface, the molecular population will change in the I_C region. To maintain the accuracy of the approximation, we consider that if a jump across an interface happens, we will reset the value of Δt_C to let the iteration run simultaneously with the jump. The details will be explained in the algorithm overview.

Algorithm overview

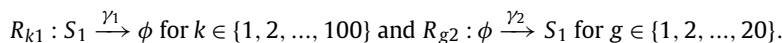
For a system in a one-dimensional domain with length L , given an initial time $t = t_0$, an initial condition $X(t_0) = X_0$ and a final time T , we perform the following steps:

1. Set a value h for the spatial size of each compartment such that the number of compartments is an integer $K = L/h$. Assign an index from $\{1, 2, \dots, K\}$ for each compartment. Set an error parameter ϵ and an interface threshold N_{int} which will be used in Eqs. (6) and (9), respectively.
2. By Eq. (6) with N_{int} , divides $\{1, 2, \dots, K\}$ into four sets of indexes I_D , I_C , I_{BL} and I_{BR} .
3. If I_C is not empty, use Eq. (9) to calculate Δt_C and set $T_C = t + \Delta t_C$; otherwise, set $\Delta t_C = T_C = \infty$ and run the SSA for the entire spatial domain until I_C is not empty.
4. If I_D is not empty, generate two independent random numbers r_1 and r_2 which are uniformly distributed in $[0, 1]$. Calculate the next reaction time $\Delta t_D = -\frac{1}{\alpha_0} \ln(r_1)$ for the SSA, where α_0 is the sum of the propensity functions of the right jumps J_{ikR} (for $k \in I_D \cup I_{BR}$), the left jumps J_{ikL} (for $k \in I_D \cup I_{BL}$) and the reactions R_{ki} (for $k \in I_D$) for $i \in \{1, 2, \dots, M\}$. Set $T_D = t + \Delta t_D$. Use the SSA method with the second random number r_2 to find the corresponding reaction or jump. If I_D is empty, set $\Delta t_D = T_D = \infty$.
5. (a) Case 1: If $T_C < T_D$, run the iteration (7) with $\Delta t = \Delta t_C$ for all the compartments in I_C . Set $t = T_C$.
 (b) Case 2: If $T_C = T_D$, run the iteration (7) with $\Delta t = \Delta t_C$ for all the compartments in I_C . Set $t = T_C$. Run the SSA for updating X in accordance with the reaction or jump found in Step 4.
 (c) Case 3: If $T_C > T_D$ and a jump across the interfaces is selected for the firing reaction in the SSA method, run the iteration (7) with $\Delta t = \Delta t_C - (T_C - T_D)$ for all i th compartment, where $i \in I_C$. Run the SSA for updating X in accordance with the reaction or jump found in Step 4. Set $t = T_D$.
 (d) Case 4: Cases 1–3 are not satisfied, update X in accordance with the reaction or jump found in Step 4. Set $t = T_D$.
6. For Cases 1, 2 and 3, reset the four sets I_{BL} , I_{BR} , I_D and I_C according to Eq. (6). If I_C is not empty, use Eq. (9) to calculate new Δt_C and set $T_C = t + \Delta t_C$; otherwise, set $\Delta t_C = T_C = \infty$. For Case 4, if I_C is empty, the similar update of the sets is needed; if I_C is not empty, the update of the sets is not needed.
7. Go back to Step 4 until $t \geq T$.

Numerical results

Linear system

Here we apply a simple linear system to compare the performance of the hybrid method with different time step settings. In the linear system, there is only one type of molecules, S_1 , in a one-dimensional domain of length $L = 50$. We divide the domain into 100 compartments with uniform size $h = 50/100 = 0.5$. There are two types of reactions listed as



The molecule S_1 diffuses with a coefficient D with reflective boundary conditions. We set $\gamma_1 = 1$, $\gamma_2 = 500$ and the diffusion coefficient $D = 10$. The initial condition for X_{k1} which represents the number of S_1 in the k th compartment is:

$$X_{k1}(0) = \lfloor 55 - 0.5k \rfloor, \text{ for } k = 1, \dots, 100.$$

For this linear system, we can explicitly obtain the exact solutions of the mean and the standard deviation, which will be used to calculate the error to verify the accuracy. Also, this type of simple model was often applied to study the stochastic effect in biological patterning [20,24].

If we use the SSA to simulate the system from $t = 0$ to $t = 6$, the average computational cost per simulation is over 60 seconds among 5,000 simulations. When we apply our hybrid method with $\epsilon = 0.1$ and $N_{int} = 10$, the computational cost is reduced to 8 second which is 13% of the cost of the SSA.

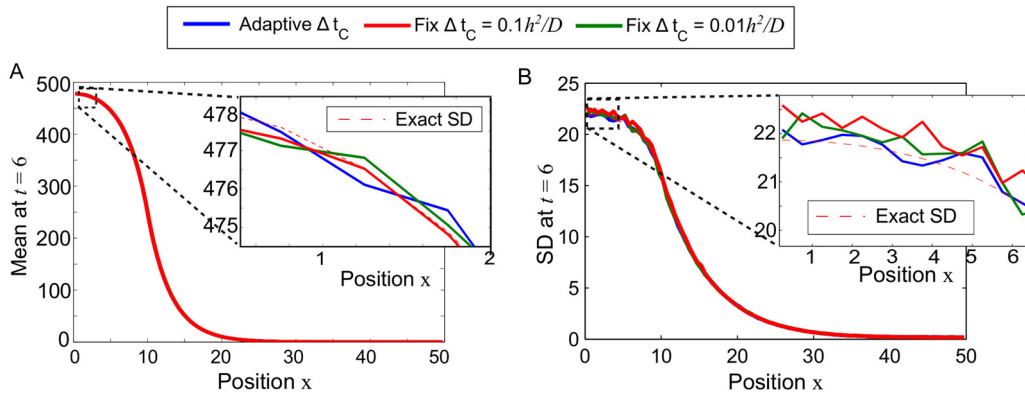


Fig. 2. The simulation results at $t = 6$ for the linear system by the hybrid method with different Δt_C settings: fixed $\Delta t_C = 0.1h^2/D$, $0.01h^2/D$ and an adaptive Δt_C defined in (9). A) The mean values of the gradients. B) The standard deviations of the gradients. For each case, 5,000 simulations are collected to obtain the statistical results. The dashed lines represent the exact solutions of the mean and the standard deviation.

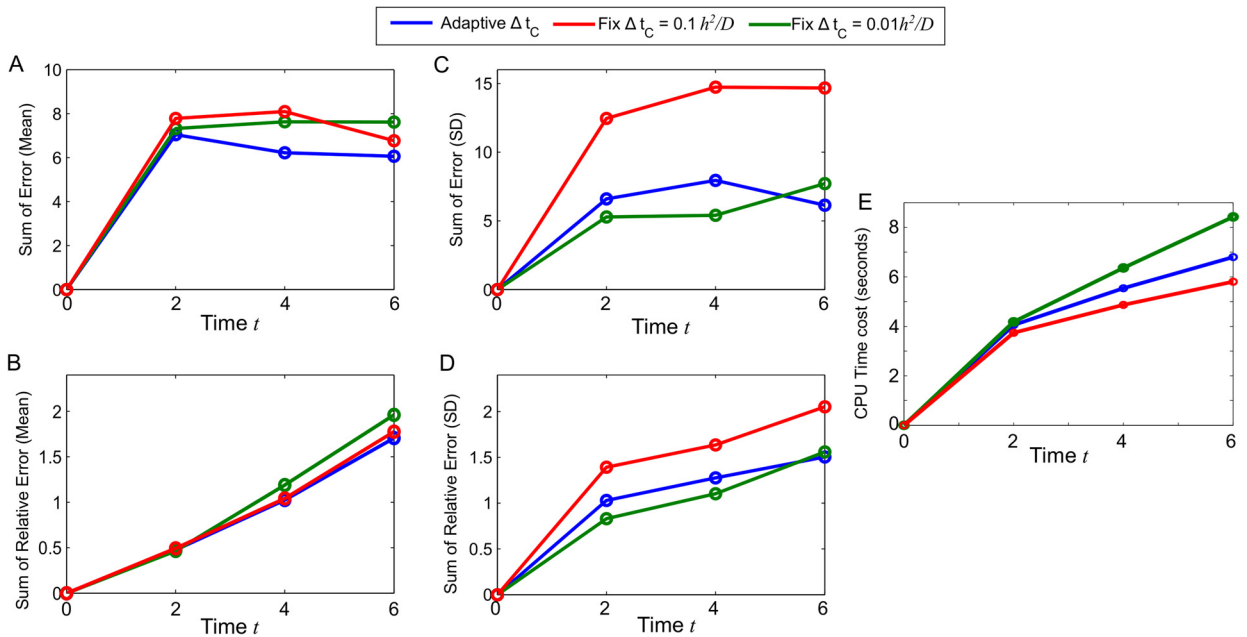


Fig. 3. The accuracy and the efficiency of the hybrid method with different Δt_C settings. A) The sums of the error of the mean. B) The sums of the relative error of the mean. C) The sums of the error of the standard deviation. D) The sums of the relative error of the standard deviation. E) The computational costs at different time t .

To show the advantage of the adaptive Δt_C , we compare the performance of the hybrid method with different Δt_C settings. Fig. 2 shows that the mean values and the standard deviations of the cases with a fixed $\Delta t_C = 0.1h^2/D$, $0.01h^2/D$ and an adaptive Δt_C defined in (9). For each case, 5,000 simulations are collected to obtain the statistical results.

Fig. 2A shows that all three cases have a similar accuracy when the solutions are compared with the exact mean solution; the standard deviations shown in Fig. 2B demonstrate that the case with a fixed $\Delta t_C = 0.1h^2/D$ does not perform as good as the other two cases. To quantify the results, we measure the sum of the error (the absolute differences between the approximation and the exact solution in each compartment) in all compartments and the results are shown in Fig. 3.

Fig. 3A shows that the sums of the error do not have a huge change with different Δt_C settings. This result is consistent when we consider the sums of the relative error (the absolute differences between the approximation and the exact solution divided by the exact solution in each compartment) shown in Fig. 3B. When we measure the error in the standard deviation (Figs. 3C, D), the case with a fixed $\Delta t_C = 0.1h^2/D$ has a larger error, also a relative error, than the other two cases which have similar performance in approximating the standard deviation. However, the efficiency of the case with a fixed $\Delta t_C = 0.1h^2/D$ is the best among all three cases (Fig. 3E). The average computational cost for this case is around 6 seconds. Between the other two cases, the adaptive time step setting has less computational cost than the case with a fixed $\Delta t_C = 0.01h^2/D$ (the former is 7 seconds per simulation and the latter is over 8 seconds per simulation) although they have similar performance in the accuracy. Compared with the SSA (60 seconds per simulation), the hybrid method with the

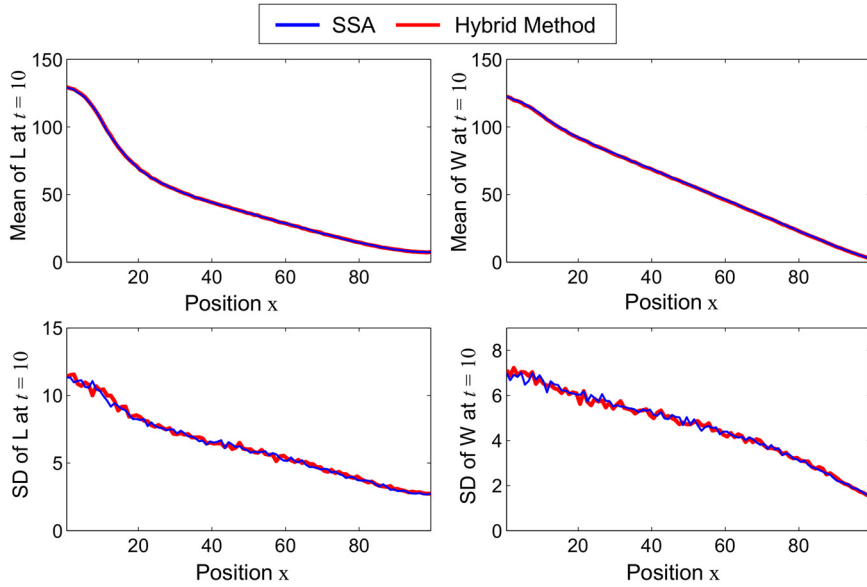
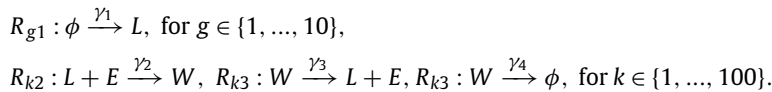


Fig. 4. The simulation results for the system of morphogen-mediated patterning by the SSA and the hybrid method with $\epsilon = 0.1$ and $N_{int} = 5$. For each case, 1,000 simulations are collected to obtain the statistical results.

adaptive time step setting saves over 80% of computational cost and provides an advantage on balancing between the accuracy and efficiency (Figs. 3C–E).

System of morphogen-mediated patterning

In [19], the system of morphogen-mediated patterning involves three types of molecules, L , E and W , which are free ligand, receptor and ligand-receptor complex, respectively. We divide the domain of length $100 \mu\text{m}$ into 100 compartments with size $h = 1 \mu\text{m}$ and a compartment represents a single cell. Free morphogens are produced in a local region $[0, 10]$ and diffuse in the domain with a diffusion coefficient $D_1 = 10 \mu\text{m}^2 \text{s}^{-1}$; receptors and ligand-receptor complexes are fixed on the cell membrane. In each compartment, the reactions are listed as



Assume that the number of total receptors is large enough, then the frustration of $E + W$ is relatively small. We simplify the system by assuming $R + W$ is a constant number $E_T = 500$ in each compartment. The parameter values are listed as follows: $\gamma_1 = 10 \text{ s}^{-1}$, $\gamma_2 = 10^{-4} \text{ s}^{-1}$, $\gamma_3 = \gamma_4 = 10^{-2} \text{ s}^{-1}$. The initial conditions for X_{k1} and X_{k2} , which represent the numbers of L and W in the k th compartment, respectively, are:

$$X_{k1}(0) = X_{k2}(0) = \lfloor 100 - k \rfloor, \text{ for } k = 1, \dots, 100.$$

Fig. 4 shows the results of the means and the standard deviations of the solutions at $t = 10 \text{ s}$, which are obtained from the SSA and the hybrid method with $\epsilon = 0.1$ and $N_{int} = 5$. For each case, 1,000 simulations are collected to obtain the statistical results. From the simulation results, we find that the hybrid method has a good performance as the SSA. On the other hand, the average computational cost of the hybrid method per simulation is 3.42 s but the average computational cost of the SSA is 15.49 s which is 4 times longer than that of the hybrid method. We also apply the hybrid method with two larger threshold values $N_{int} = 10$ and $N_{int} = 20$ and find that the accuracy does not have any significant change but the computational cost increases from 3.42 s to 8.74 s when N_{int} increases from 5 to 20. Moreover, when the smaller $N_{int} = 2$ is considered, the computational cost increases from 3.42 s to 5.29 s as a smaller time step Δt_C is required for maintaining the accuracy of the approximation when N_{int} decreases. Compared with the SSA, the hybrid method with a suitable N_{int} can save over 75% of computational cost for this simulation.

System of yeast polarity

In [1], the stochastic model of cell polarization showed that a positive feedback alone is sufficient to account for the spontaneous establishment of a single site of polarity. We apply the model in [1] to verify the accuracy of our method. In

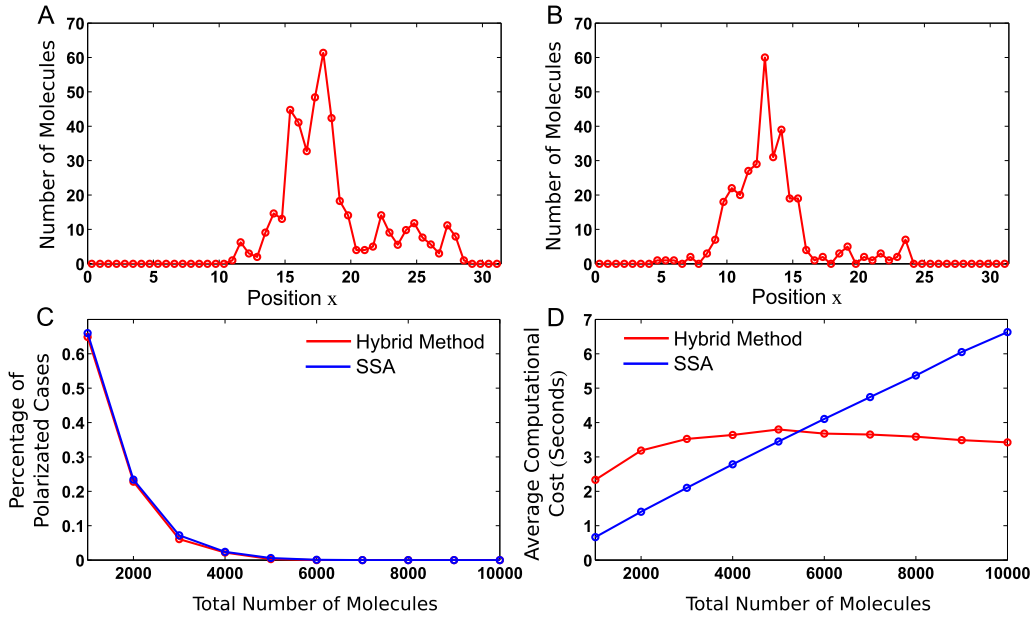
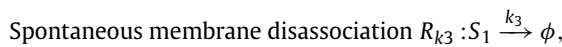
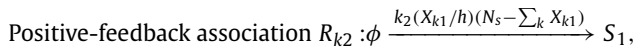


Fig. 5. The accuracy and the efficiency of the hybrid method with different numbers of signaling molecules N_s . A) A sample simulation at $t = 20$ min through the hybrid method with $N_s = 4000$. B) A sample simulation at $t = 20$ min through the SSA method with $N_s = 4000$. C) The percentage of polarized cases within 1,000 independent simulations for different N_s values. D) The average computational cost within 1,000 independent simulations for different N_s values.

the model, there is only one type of signaling molecules, S_1 , and the computational domain represents the cross section of cell membrane which is considered as a one-dimensional domain with length $10\pi \mu\text{m}$ (the radius of cell is $5 \mu\text{m}$). The domain is partitioned into 50 identical compartments with uniform length $0.2\pi \mu\text{m}$. Signaling molecules move between cytoplasmic states and membrane-bound states. In each compartment, there are three types of reactions: spontaneous membrane association (from cytoplasmic state to membrane-bound state), positive-feedback association (from cytoplasmic state to membrane-bound state) and spontaneous membrane disassociation (from membrane-bound state to cytoplasmic state). Let X_{k1} be the number of S_1 in the k th compartment. In each compartment, we have



with the propensity functions

$$\alpha_{k1} = k_1(N_s - \sum_k X_{k1}),$$

$$\alpha_{k2} = k_2(X_{k1}/h)(N_s - \sum_k X_{k1}) \text{ and } \alpha_{k3} = k_3 X_{k1},$$

where N_s is the total number of signaling molecules. The initial condition is $X_{k1} = 10$ for all k . For our hybrid method, we set $\epsilon = 0.1$ and $N_{int} = 5$; for the biological parameters, we set $D = 1.2 \mu\text{m}^2/\text{min}$, $k_1/k_2 = 10^{-4}$, $k_3 = 9/\text{min}$ and $k_2/k_3 = 0.9N_s$ [1]. The initial condition for S_1 is

$$X_{k1}(0) = \lfloor 10\delta_k \rfloor, \text{ for } k = 1, \dots, 100,$$

where δ_k 's are independent random numbers generated from the uniform distribution on $[0, 1]$. Figs. 5A and B show two sample simulations at $t = 20$ min, obtained by the hybrid method and the SSA, respectively.

In [1], the stochastic model of cell polarization demonstrated that the frequency of polarization inversely depends on the number of signaling molecules N_s . Figs. 5C and D show that the hybrid method and the SSA can capture this feature of the system. We assume that polarization in simulations at $t = 20$ min is determined by whether an interval of 10% of the whole domain contains more than 50% of the total number of signaling molecules (as the samples in Figs. 5A and B). Fig. 5C shows the percentage of polarized cases within 1,000 independent simulations for different N_s values (red line represents the hybrid method; the blue line represents the SSA). The frequency of polarization is decreasing from 0.65 to 0 when the number

of signaling molecules is increasing from 1,000 to 10,000. For the case with too many signaling molecules, the molecules may be able to form more than one clusters at the same time so a single site of polarity cannot be achieved. This result is consistent with the experimental observation of yeast cells [1]. This phenomenon was not observed in the deterministic models so it may support that the randomness plays an important role in the process of cell polarization. For studying the efficiency, when the number of signaling molecules N_s increases from 1,000 to 10,000, the average computational cost for the SSA increases from 0.7 seconds to 6.6 seconds (Fig. 5D, the blue line); the average computational cost for the SSA does not change a lot and is stable around 3.5 seconds (Fig. 5D, the red line). These results show that the hybrid method has an advantage that the computational cost for the simulation does not depend on the number of molecules involved. Moreover, the result in Fig. 5D also shows that our hybrid method performs better when the number of the molecules increases (the computational cost is reduced to around 50% of the cost of the SSA when the number of the molecules is 10,000) since the approximation of the numerical SDE can speed up the simulation process in the region of high concentration.

Conclusion

In this paper, we have developed a hybrid method which combines the SSA and numerical SDE with an adaptive time step control. The design principle of this method is to take advantage of strengths in both methods: the SSA is accurate when the numbers of molecules are small, and the numerical SDE is efficient when the numbers of molecules are large.

The numerical results showed that our hybrid method provided a good agreement for the first two moments and could save the computational cost over 80% when a large number of molecules are involved in the system. The time step control in (9) provides an adaptive way to decide the time step size for the numerical SDE to bound the error in the approximations of the means and standard deviations. Our results in Fig. 3 showed that the hybrid method with the adaptive time step control provides a better balance between the accuracy and the efficiency than using fixed time step.

Although our hybrid method was shown to have a relatively high efficiency in some simulations, certain results (Fig. 5) show that our method may need more computational cost than the SSA when the number of molecules involved is relatively small. For improving the efficiency, several improvements can be made for further development. In our simulations, we found that the computational cost may increase when the threshold N_{int} is too small or too large, so it is important to develop a method to determine a value for N_{int} for optimizing the performance of our method. Also, although our method performed very well for some one-dimensional systems, the performance may not be better than the SSA for two- or three-dimensional systems. In a higher dimensional domain, we have to consider one- or two-dimensional interfaces for separating the two approaches. The increase of the dimension of the interfaces may cause frequent occurrences of stochastic jumps across the interfaces. In our setting, we consider that if a stochastic jump across an interface happens, we will reset the value of Δt_C to let the iteration of the numerical SDE occur at the same time of the stochastic jump. So the frequent occurrence of a stochastic jump may reduce the efficiency of our method. However, a jump of a molecule may not cause a significant change in the reaction rates when N_{int} is relatively large. According to this observation, we can relax this condition by defining a threshold value N_j and considering that if stochastic jumps across the interfaces happen more than N_j times at same location, we will reset the value of Δt_C to let the iteration occur simultaneously. Overall, our hybrid method provides a framework for further development of full stochastic hybrid methods, for example, by coupling with the Brownian dynamics simulations [11,26,29] and the τ -Leaping strategy [6,7,10,25].

Acknowledgements

We are grateful to Dr. Louis Fan for his useful discussion. This research was supported by a grant from the Research Grants Council of the Hong Kong Special Administrative Region, China (Project No. CityU 21303615).

References

- [1] S.J. Altschuler, S.B. Angenent, Y. Wang, L.F. Wu, On the spontaneous emergence of cell polarity, *Nature* 454 (2008) 886–889.
- [2] G. Balázs, A. van Oudenaarden, J.J. Collins, Cellular decision making and biological noise: from microbes to mammals, *Cell* 144 (2011) 910–925.
- [3] T. Bollenbach, P. Pantazis, A. Kicheva, C. Bokel, M. Gonzalez-Gaitan, F. Julicher, Precision of the Dpp gradient, *Development* 135 (2008) 1137–1146.
- [4] K. Burrage, I. Lenane, G. Lythe, Numerical methods for second-order stochastic differential equations, *SIAM J. Sci. Comput.* 29 (2007) 245–264.
- [5] Y. Cao, D.T. Gillespie, L.R. Petzold, Efficient step size selection for the tau-leaping simulation method, *J. Chem. Phys.* 124 (2006) 044109.
- [6] Y. Cao, D.T. Gillespie, L.R. Petzold, Adaptive explicit–implicit tau-leaping method with automatic tau selection, *J. Chem. Phys.* 126 (2007) 224101.
- [7] Y. Cao, D.C. Samuels, Discrete stochastic simulation methods for chemically reacting systems, *Methods Enzymol.* 454 (2009) 115–140.
- [8] K.H. Chiam, C.M. Tan, V. Bhargava, G. Rajagopal, Hybrid simulations of stochastic reaction–diffusion processes for modeling intracellular signaling pathways, *Phys. Rev. E, Stat. Nonlinear Soft Matter Phys.* 74 (2006) 1.
- [9] A. Eldar, M.B. Elowitz, Functional roles for noise in genetic circuits, *Nature* 467 (2010) 167–173.
- [10] L. Ferm, A. Hellander, P. Lötstedt, An adaptive algorithm for simulation of stochastic reaction–diffusion processes, *J. Comput. Phys.* 229 (2010) 343–360.
- [11] B. Franz, M.B. Flegg, S.J. Chapman, R. Erban, Multiscale reaction–diffusion algorithms: PDE-assisted Brownian dynamics, *SIAM J. Appl. Math.* 70 (2013) 1224–1247.
- [12] D.T. Gillespie, A general method for numerically simulating the stochastic time evolution of coupled chemical reactions, *J. Comput. Phys.* 22 (1976) 403–434.
- [13] J.U. Harrison, C.A. Yates, A hybrid algorithm for coupling partial differential equation and compartment-based dynamics, *J. R. Soc. Interface* 13 (2016) 20160335.
- [14] J. Hu, H.W. Kang, H.G. Othmer, Stochastic analysis of reaction–diffusion processes, *Bull. Math. Biol.* 76 (2014) 854–894.

- [15] S.A. Isaacson, C.S. Peskin, Incorporating diffusion in complex geometries into stochastic chemical kinetics simulations, *SIAM J. Sci. Comput.* 28 (2006) 47–74.
- [16] G. Kalantzis, Hybrid stochastic simulations of intracellular reaction–diffusion systems, *Comput. Biol. Chem.* 33 (2009) 205–215.
- [17] H.-W. Kang, L. Zheng, H.G. Othmer, A new method for choosing the computational cell in stochastic reaction–diffusion systems, *J. Math. Biol.* 65 (2012) 1017–1099.
- [18] P.E. Kloeden, E. Platen, *Numerical Solution of Stochastic Differential Equations*, Springer, 1992.
- [19] A. Lander, Q. Nie, F.Y.M. Wan, Do morphogen gradients arise by diffusion?, *Dev. Cell* 2 (2002) 785–796.
- [20] A.D. Lander, W.C. Lo, Q. Nie, F.Y.M. Wan, The measure of success: constraints, objectives, and tradeoffs in morphogen-mediated patterning, *Cold Spring Harb. Perspect. Biol.* 1 (2009) a002022.
- [21] M.J. Lawson, B. Drawert, M. Khammash, L. Petzold, T.-M. Yi, Spatial stochastic dynamics enable robust cell polarization, *PLoS Comput. Biol.* 9 (2013) 1–12.
- [22] J. Lei, Stochasticity in single gene expression with both intrinsic noise and fluctuation in kinetic parameters, *J. Theor. Biol.* 256 (2009) 485–492.
- [23] W.-c. Lo, L. Zheng, Q. Nie, A hybrid method for stochastic reaction–diffusion processes, *R. Soc. Open Sci.* 3 (2016) 160485.
- [24] W.-C. Lo, S. Zhou, F.Y.-M. Wan, A.D. Lander, Q. Nie, Robust and precise morphogen-mediated patterning: trade-offs, constraints and mechanisms, *J. R. Soc. Interface* 12 (2014) 20141041.
- [25] J.M.A. Padgett, S. Ilie, An adaptive tau-leaping method for stochastic simulations of reaction–diffusion systems, *AIP Adv.* 6 (2016) 035217.
- [26] M. Robinson, M. Flegg, R. Erban, Adaptive two-regime method: application to front propagation, *J. Chem. Phys.* 140 (2014) 124109.
- [27] D. Rossinelli, B. Bayati, P. Koumoutsakos, Accelerated stochastic and hybrid methods for spatial simulations of reaction–diffusion systems, *Chem. Phys. Lett.* 451 (2008) 136–140.
- [28] C.A. Smith, C.A. Yates, Spatially extended hybrid methods: a review, *J. R. Soc. Interface* 15 (2018) 20170931.
- [29] C.A. Smith, C.A. Yates, The auxiliary region method: a hybrid method for coupling PDE- and Brownian-based dynamics for reaction–diffusion systems, *R. Soc. Open Sci.* 5 (2018) 180920.
- [30] F. Spill, P. Guerrero, T. Alarcon, P.K. Maini, H. Byrne, Hybrid approaches for multiple-species stochastic reaction–diffusion models, *J. Comput. Phys.* 299 (2015) 429–445.
- [31] C. Ta, D. Wang, Q. Nie, An integration factor method for stochastic and stiff reaction–diffusion systems, *J. Comput. Phys.* 295 (2015) 505–522.
- [32] N.G. Van Kampen, *Stochastic Processes in Physics and Chemistry*, vol. 1, Elsevier, 1992.
- [33] L. Zhang, K. Radtke, L. Zheng, A.Q. Cai, T.F. Schilling, Q. Nie, Noise drives sharpening of gene expression boundaries in the zebrafish hindbrain, *Mol. Syst. Biol.* 8 (2012) 613.